Experience and Learnings with Inclined Anode Slots in High Amperage Aluminium Reduction Cell

Alexandre Blais[1] and Pascal Thibeault[2]
1. Project Leader Reduction
2. Principal Advisor Creeping & Lining
Rio Tinto – Arvida Research and Development Centre, Saguenay, Canada
Corresponding author: alexandre.blais@riotinto.com
https://doi.org/10.71659/icsoba2024-al042

Abstract

Rio Tinto is known for its high amperage operation and its main primary aluminium production hub in the Saguenay Lac Saint-Jean region (Québec, Canada), with five aluminium smelters and a research centre. Over the last decades, cell designs have continuously evolved to allow higher heat dissipation and support successive amperage increases. Recently, a recurring problem threatening cell life duration, expressed by repetitive shell sidewall temperature peaks, was encountered in one of the regional smelters. The situation was addressed by mobilizing R&D teams to understand the provenance of the phenomenon taking place and to propose a solution to mitigate it. The results of the investigations pointed to a solution lowering the solicitation of the inner sidewalls of the cell by modifying the anode slot design. Industrial tests were carried out using different anode slot designs to better assess the behaviour of the proposed solution. The retained inclined anode slot design has been in operation for more than two years now.

This paper presents the sequence of events that unfolded from the apparition of the problem to its solution. It summarizes the experience gathered through key learnings in both technical and operational fields. It also addresses the thermal impact that needs to be compensated in the operation of the cells with the new anode slot design.

Keywords: Aluminium reduction cell, Anode slots, Cell sidewall, Cell ledge.

1. Introduction

Rio Tinto is a large aluminium producer operating different aluminium reduction technological platforms, with most of its production located in the Saguenay region (Québec, Canada). Rio Tinto also benefits from two private R&D centres which support the continuous improvement of technologies. Thanks to sustained developments over the last two decades, a growth of 1 % per year on amperage has been achieved, bringing local production to more than 1.2 million tonnes of aluminium per year.

The AAR-AP60 smelter (Aluminerie Arvida, Centre Technologique AP60) started in 2013 as a highly productive technology, maximizing the size of the shell and anodes, to produce more than 20.5 tonnes of aluminium per year per cell square meter. This technology is currently in the validation phase, with a cell configuration that defines new limits, exacerbating certain phenomena detrimental to performance. During the test phase, the repeated appearance of hot spots on the long sidewalls of the cells was observed. The R&D teams followed an exhaustive approach to understand and resolve the problem on a group of pilot cells before generalization. The use of inclined anode slots, increasingly

found throughout the aluminium industry, is the main solution. The various tests carried out provided a better understanding of how they work and their advantages and disadvantages.

1.1 Anode Slots in Aluminium Production: A Brief Review

The Hall-Héroult process uses a reactor, or aluminium reduction cell, to feed alumina (aluminium oxide) into a high temperature melted cryolite bath, where it is transformed into aluminium by the passage of direct electric current following reaction (1).

$$2\,Al_2O_3 + 3\,C = 4\,Al + 3\,CO_2 \quad (1)$$

The electrical power fed to the cell (voltage times amperage) is used to preheat raw materials and to carry out the alumina reduction while the rest (roughly 50 %) is dissipated as heat through exchanges with the cell surroundings. There exists an operating power range for each cell design within which a sufficient layer of frozen bath forms inside the cell, protecting the lining from the corrosive bath to ensure the long-term operation of the cell (cathode blocks erosion as the expected failure mode). The reduction of aluminium oxide, equation (1), also produces carbon dioxide bubbles, combining oxygen from the alumina with carbon from the anodes. The continuous generation of this gas phase creates movements in the liquid bath, which enhances alumina dissolution and heat transfer in the cell. Buoyancy keeps the bubbles at the anode bottom surface, where they form an electrically insulative layer, referred to as "bubble voltage" in operating terms. The longer the gas bubbles stay under the anodes, the more likely they are to coalesce, forming larger bubbles which can insulate parts of the anode surface, increasing the cell electrical resistance.

To better understand and ultimately predict the "bubble voltage", studies were carried out on the behaviour of the bubbles themselves, from physical air-water models to computational fluid dynamics modelling [1, 2]. To shorten the residence time of the bubbles under the anodes, by reducing their mean free path, the anode bottom surface was slit with perpendicular grooves, or slots. Many slot designs have been studied [1, 3, 4, 5], but the ones running along the long side of the anode block offer better results in terms of reducing gas coverage and voltage [1, 2, 5, 6]. Such longitudinal slots are thus common within the aluminium industry nowadays, as they reduce the noise of the cell (or cell resistance variation) by reducing the current variation of individual anodes compared to non-slotted anodes [7].

The discharge of the gases collected in the slots occurs differently if the slot height reaches above the bath level (slot partly immersed in the bath) or if the slot is completely immersed in the bath. When a new anode is set, part of its slots is outside the bath, provided that they are higher than a certain height (i.e., slot height greater than "bath height minus ACD", where ACD is anode-to-cathode distance). As the carbon anode is consumed, the slots become fully immersed in the bath, drastically changing the behaviour of the generated gases and their impact on the cell, as shown on Figure 1, until the slots disappear. In the former case, the gas bubbles escape through the free bath surface, causing smaller bath displacements. In the latter case, the captured gases are ejected along the channel formed by the slots, causing bath displacement at both ends (lateral and central channels of the cell). In the central channel, these movements are linked with stirring and improved dissolution [2, 7], while in the lateral channel, they foster advection effects onto the inner sidewall [5, 8, 9].

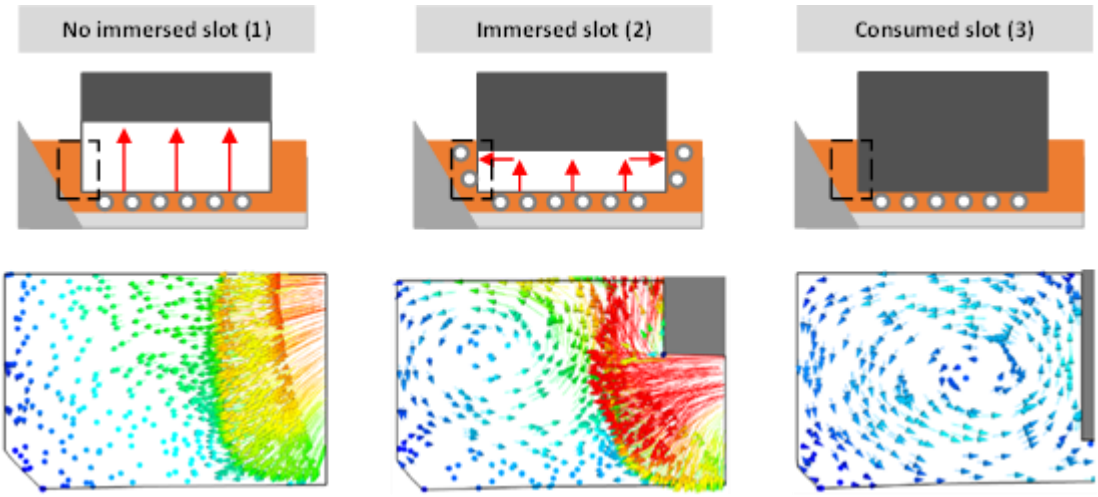

Figure 1. Gas and bath mixture velocity in the anode slot for three cases (adapted from [9]).

An increased heat transfer from the ejection of the gas bubbles in the case of fully immersed anodes is also pointed out by [5], which suggests coupling Computational Fluid Dynamics (CFD) and Finite Elements Method (FEM) to obtain the impact on the cell's ledge protection. Such a study has been carried out by [8], importing heat transfer coefficients calculated from CFD modelling into an FEM model to assess the impact of the bubbles on the ledge protection, which is weak in the case they studied. A more complete approach is taken in [9] where the Alucell software (a set of models to compute the Magnetohydrodynamic (MHD)-induced movements and displacement of the metal, coupled with a thermo-electrical balance evaluating ledge protection) is upgraded with a CFD model to consider the gas bubbles and the anode slot configuration. In addition to the results in Figure 1, they present other results explaining the temporal behaviour of a temperature trace on the shell sidewall, which increases when the anode slots become fully immersed. They also detail the differences between upstream and downstream shell sidewall temperature signals (from measurements), and between upstream and downstream ledge thicknesses (from model predictions), based on the MHD-driven metal flow in AP6X cells [10].

As explained in [5], one might design anode slots to take advantage of the enhanced bath mixing they create once submerged. This is attained using slots inclined towards the central channel, promoting bath mixing and alumina dissolution in this region while lowering bath mixing in the lateral channel, favouring a stable inner sidewall ledge protection [4]. The angle and the thickness of the slots are shown to have an impact on the evacuation of gases in their immersed phase [5].

2. Problem: Recurring Red Spots on the Shell Sidewall

The booster section at the AAR-AP60 smelter is used to prepare the future operating point of the whole line, at an amperage above 600 kA. The setup for the current development was put in place at the end of 2020, with a new cell design to support the amperage increase. Figure 2 presents a high-level timeline going from early 2021 to the present day. It is noteworthy that the booster section only operated a few months near its 24 kA target between September 2021 and October 2023. The problem that brought these delays lead R&D teams to develop knowledge and identify a technical solution. The resulting sequence of events is the subject of this paper.

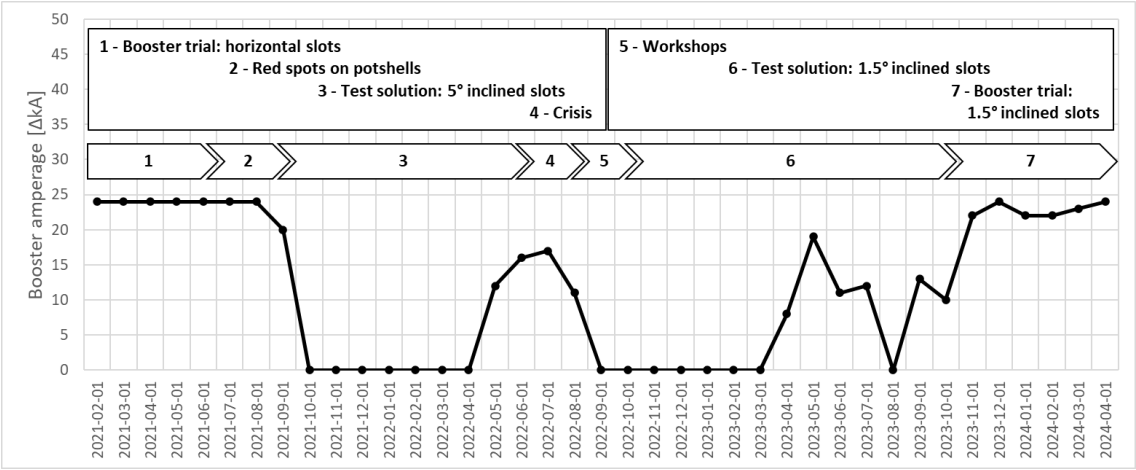

Figure 2. AAR-AP60 booster trial timeline.

2.1 Particularities of the AP6X Cell Design

Comparing the actual AP6X cell design to the first generation of AP60 cells [11], the former has an enlarged shell, longer anodes, and a different inner sidewall lining. Two indicators can be used to illustrate how the AP60 / AP6X platform is stretched compared to previous technologies: the *anode-to-sidewall distance* (ASD), and the "equivalent slot gas load". The ASD, which is presented on the left-hand side of Figure 3, is a dimension representing how much free space there is between the anode edge and the sidewall lining facing it. The indicator displayed on the right-hand side of Figure 3 represents the gas load per slot, expressed as an equivalent load through the units of "kA per slot", since amperage is proportional to metal production at constant current efficiency. The most salient feature of Figure 3 is the gap between older technologies (P155 and AP40) and the more recent AP6X platform.

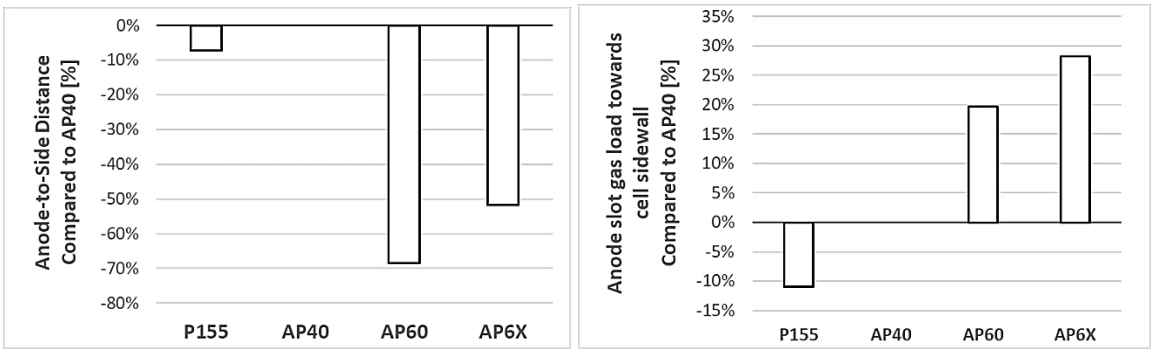

Figure 3. Benchmarking, comparing to AP40 (left: ASD, right: kA per slot).

Another design characteristic of the AP6X cell design worth mentioning is a common trait between AP4X and AP6X platforms, as the MHD-induced metal flow tends to create local zones of lesser ledge protection in upstream corners and at the downstream center [9, 10].

2.2 Shell Sidewall Temperature

As part of the high amperage development, experimental cells have been fitted with thermocouples on the shell outer sidewalls to measure temperature, with the aim of characterizing the global

temperature behaviour of the shell over time. Figure 4 shows temperature signals measured on both the upstream and the downstream sides of a booster cell for a six months period. The thermocouples are located at a sensible area on the shell, at a height facing the molten bath layer (details given in Figure 4). These signals present a common trend, independent of the date, but with a period corresponding to the anodic cycle. The intensity of the temperature peaks should also be noticed, between 150 °C and 250 °C, as it characterizes the AP6X cell design. Such regular shell temperature peaks associated with the anodic cycle were also seen on the previous generation of AP60 cells, but at a lower intensity, such that they were never investigated in detail.

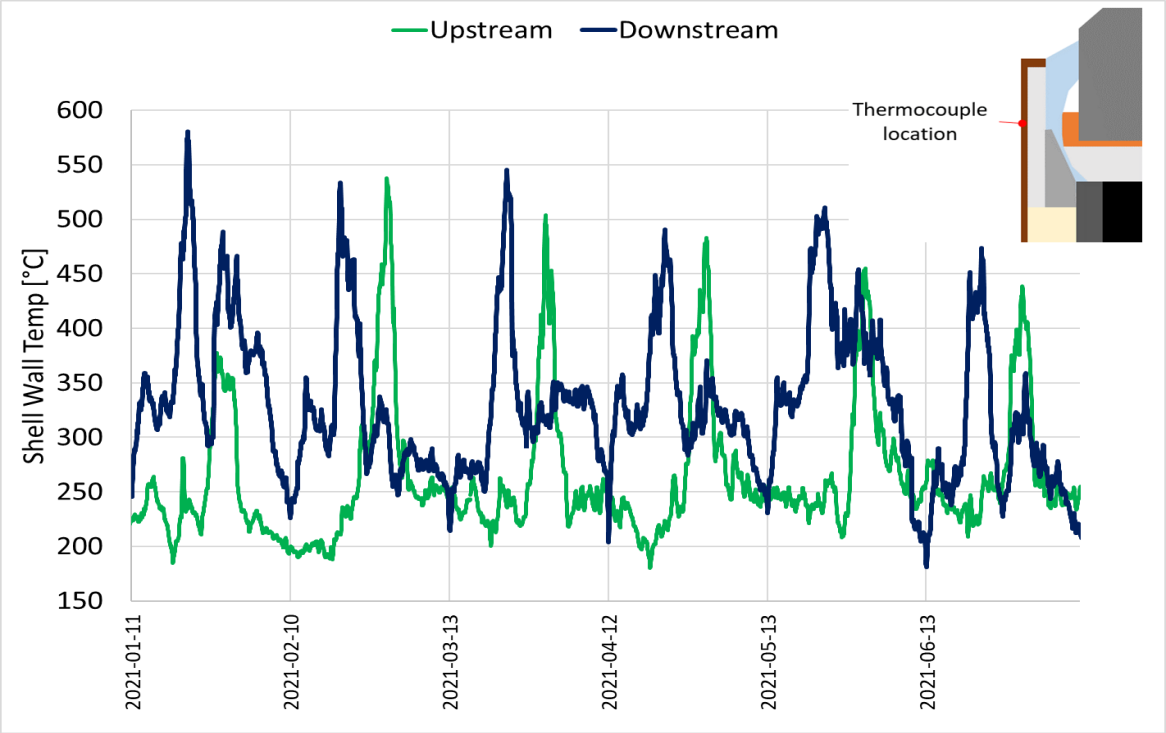

Figure 4. Shell sidewall temperature signals on a booster cell.

It is understood that the combination of the particularities of the AP6X cell design, namely the low ASD and the high gas load per slot, plays an important role for the shell sidewall temperature behavior. These add up to the MHD-induced flow pattern, which also contributes to the non-uniformity of the ledge protection within the AP6X cell. Overall, the sharp temperature increases repeatedly recorded on booster cells are indicative of significant changes in the local sidewall heat flux, temporarily melting part of the ledge protection.

2.3 Recurring Red Spots

In April 2021, having operated the booster at its target with otherwise well-behaved AP6X cells for a few months, a first red spot was observed in the booster, as shown in Figure 5. It was considered an occasional event when it occurred, and a compressed air lance was used to blow onto the shell from the outside, making the red spot disappear. However, the R&D technicians and the AAR-AP60 reduction technical group soon found other red spots the following weeks on the other booster cells. Therefore, a new routine was added for the operators and the R&D technicians to look at the booster cells' sidewalls to capture any red spot as soon as it appeared.

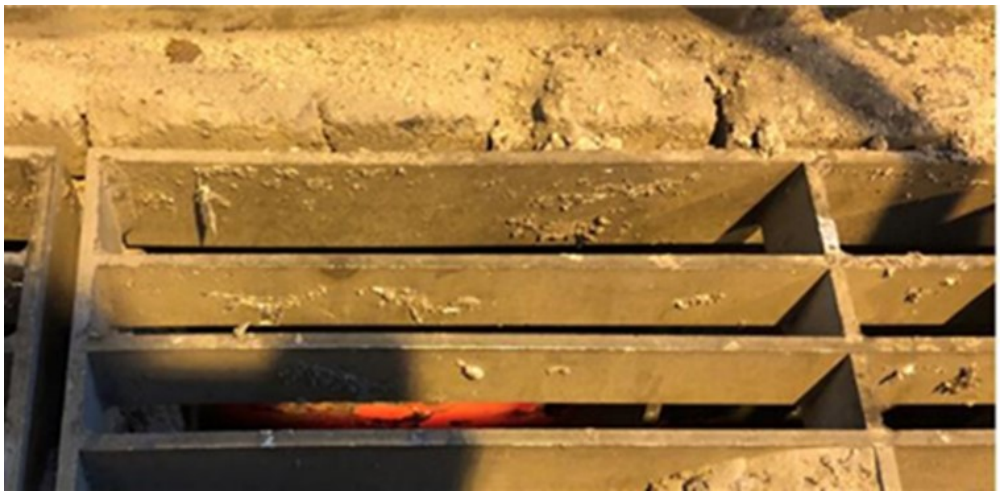

Figure 5. Red spot on the shell of a booster cell in 2021 at AAR-AP60.

Table 1 reports the red spot events that have been recorded for one of the AP6X booster cells. Two features are striking from the recorded events: first, the time interval between them (per anode position), and second, the age of the anodes facing the detected red spots. The first feature closely corresponds to the anode cycle length, while the second feature corresponds to the disappearance of the 200 mm-high slots (from an estimated carbon consumption of 20 mm per day).

Table 1. Red spot occurrences on a booster cell.

Date	Anode Position: Downstream Centre (Towards Tapping)	Anode Position: Downstream Centre (Towards Ventilation)	Anode Age (days)
2021-04-27		Red Spot	10
2021-05-28		Red Spot	11
2021-07-13	Red Spot		11
2021-08-27		Red Spot	10
2021-09-13	Red Spot		11
2021-09-27		Red Spot	10

Another important feature, implicit from Table 1, is that no recurring red spot was ever seen at any other anode position around the cells. It should also be noted that the instrumentation, although it is strategically placed onto the shell sidewall, is not always picking up a signal intensity corresponding with steel reddening (> 550 °C). This is because a single thermocouple is tapped onto a meter-wide sidewall surface, at a predefined height, facing chosen anode positions around the cell (roughly 75% of anode positions are instrumented); however, it might not be facing the exact location where the maximum temperature is attained.

Hence, as of September 2021, the amperage of the booster unit was shut down and the booster section started operating at line amperage (see Figure 2). Furthermore, a few months after the first red spot was seen in the booster section, red spots started appearing on the shells of line cells, at the same anode positions; therefore, the “red spot routine” was extended to the whole smelter. Red spots have been reported in the literature recently [12], and it is the authors’ hypothesis that the mechanism detailed in the present paper is also at play for this other case.

2.4 Understanding the Provenance of Red Spots: Horizontal Slots

Following a scientific approach, process data were analyzed to eliminate sources (booster cells' settings, smelter operations, raw materials, etc.). As temperature signals from booster cells were plotted against time, as in Figure 4, an important observation was made: all sidewall temperature traces displayed an "anodic cycle-long pattern" between temperature peaks, independently of the position of the thermocouples on the long sides of the shell (i.e., independently of anode position). This showed that red spots were "the tip of the iceberg", and that a regular phenomenon was occurring throughout the cells, but at a different intensity depending on the location. It was also observed that the shell sidewall temperature fluctuations are more important at the position representing the mid-height of the bath level, where the inner sidewall is facing the immersed part of the anode block (facing the slots, if present). This observation is consistent with the work of [5], and work cited therein, which report a recirculation zone in the cell lateral channel at a position of roughly two thirds of the total bath height.

As described in section 1.1, slotted anodes are widely used in the aluminium smelting industry. When the anodes are consumed, three distinct phases can be described (see Figure 1):

1. The top of the anode slot is above bath level
2. Immersed anode slot
3. No more slot (slotted part of the anode is fully consumed).

The findings made by R&D teams are summarized in Figure 6. The graph presents a cell sidewall temperature signal in relation to the height of the horizontal slots at the anode position facing the recorded instrumentation point. It is seen that the temperature drops when the anode is changed, resulting from the introduction of a cold anode, which corresponds to maximum slot height. Then, the sidewall temperature remains relatively constant until it increases rapidly during the period when the horizontal slot is fully immersed (slot heights of 150 mm and below). Finally, once the slots vanish, the sidewall temperature recovers (slot height at zero).

The mechanism of the anode slots' dissapearance and its impact on the shell sidewall temperature behaviour just explained is seen twice in Figure 6. For two different slot heights, the temperature peak is strongly affected by this height: with lower slots, the temperature peak happens sooner in the life of the anode, since the moment of full immersion also comes sooner, as compared to higher slots. This change in anode slot height and the ensuing sidewall temperature response are strongly suggesting that the correct physical phenomena were identified.

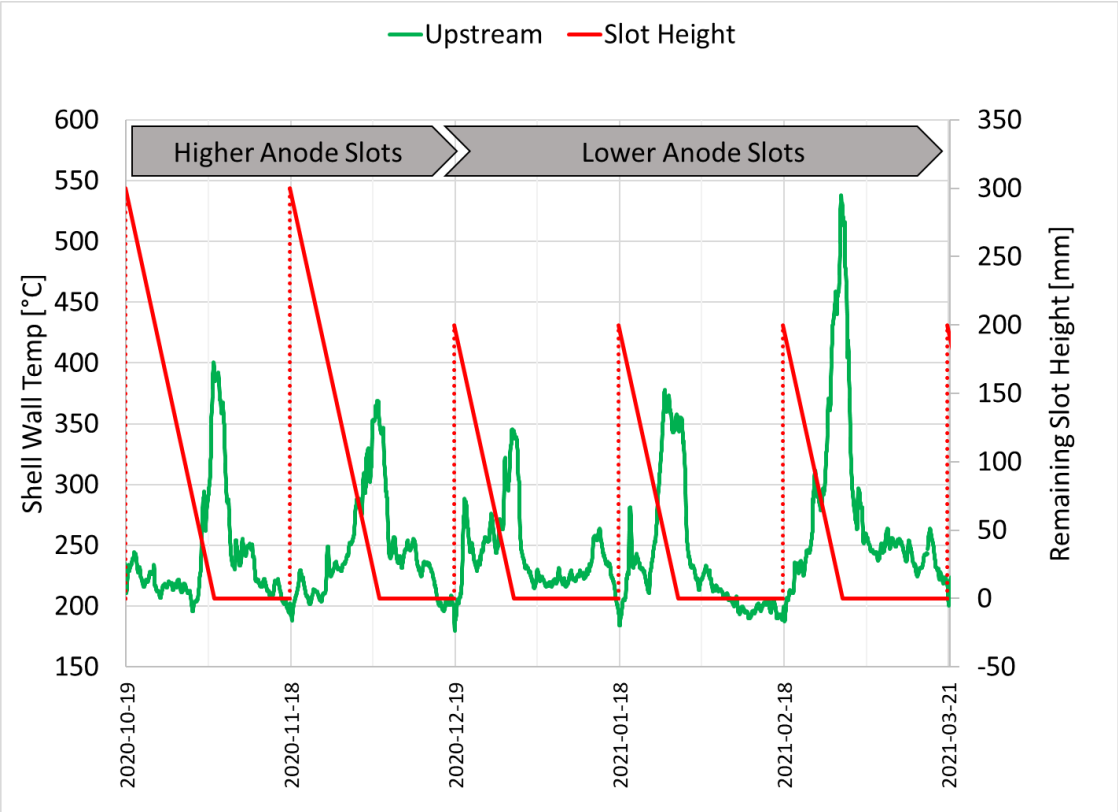

Figure 6. Cell sidewall temperature signal and anode slot height, for two different heights.

The interpretation of the temperature signals agrees well with the physics described in modeling works [5, 9]. For the AP6X technology, it represents an obvious risk of premature wear of the shell sidewalls, potentially leading to sidewall burst and early cell stoppage.

3. Solution: Inclined Slots to Lower Heat Transfer Towards Side Channel

To eliminate the recurring sidewall temperature peaks, and their negative influence on ledge protection, the strategy is to reduce the heat flux in the vicinity of the inner sidewall by changing the anode slot design, from horizontal to inclined. The slots were thus tilted to direct the gas flow towards the center of the cell. Figure 7 presents the designs of inclined slots tested in the booster section at AAR-AP60.

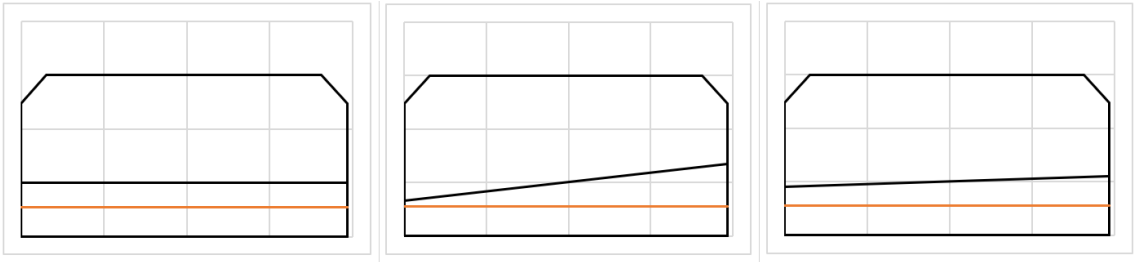

Figure 7: Anode block schematics showing: A horizontal slot (left), an inclined slot at 5 ° (center), an inclined slot at 1.5 ° (right), and the initial bath immersion (orange line)

As the R&D team's primary objective was to eliminate recurrent shell sidewall temperature peaks, the 5 ° slot was chosen at first, to force the flow of gases towards the cell center. At small angles, one might have to consider the non-horizontal placement of the anode assembly inside the cell, or some imperfection from rodding, to ensure that the gas flow is oriented as desired. Such issues were put aside by using 5 ° slots.

3.1 Improved Behaviour: Sidewall Temperature and Ledge Protection

After the booster cells conversion to inclined slots, the periodic shell sidewall temperature peaks disappeared, confirming the correct identification of the mechanism at play. This situation is depicted in Figure 8, where the sidewall temperature signals recorded for both types of anode slots are plotted over a six-month period (non-consecutive periods). With inclined slots, there is no clear pattern of the temperature signal over time, and the range of the temperature fluctuations is quite smaller.

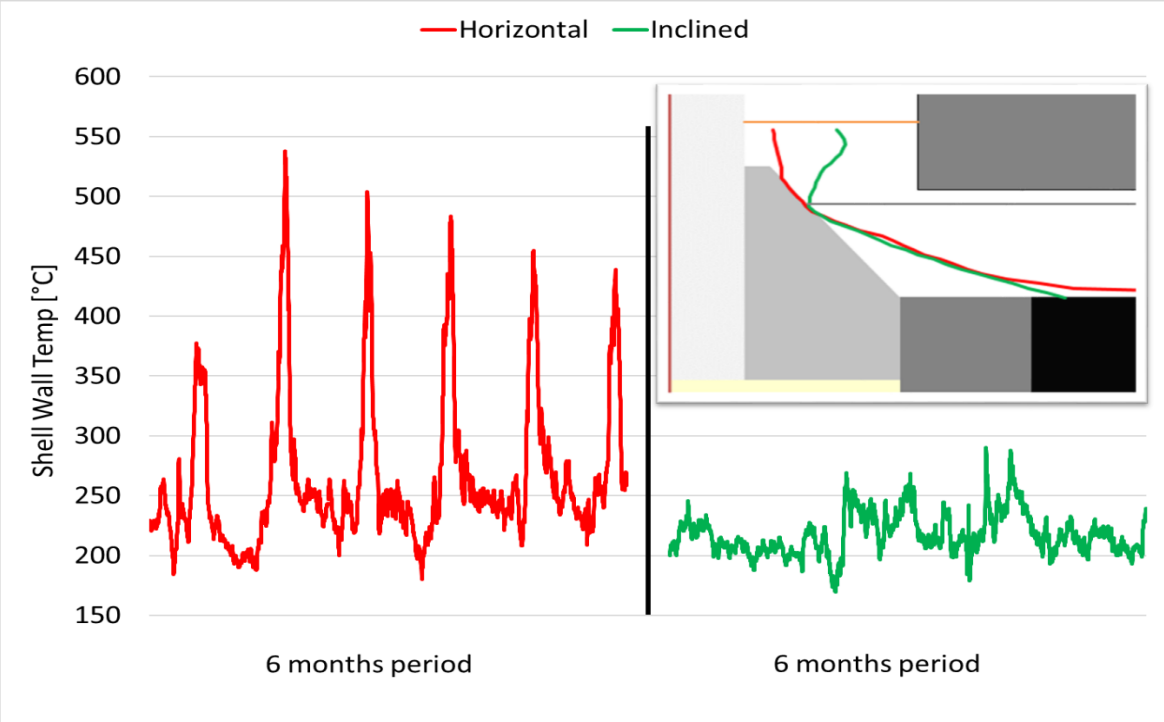

Figure 8. Effect of inclined slots on outer shell sidewall temperature and inner ledge profile.

As the shell sidewall temperature is an indication of the events occurring inside the reduction cell, intrusive measurements were carried out to evaluate the thickness of the ledge profile in front of a given anode position by removing the corresponding anode assembly. The measurements were located in the most thermally sensible part of the cell, the downstream center, and they are reported as a superimposed graph on the upper right-hand side of Figure 8. These measurements were carried out at the moment corresponding to the sidewall temperature peak: for 200 mm-high slots, it is around ten days (see Table 1). The most striking feature is the difference in ledge protection between the two anode slot designs in the bath layer (i.e., between the horizontal lines on the inset graph, which represent the metal and the bath surfaces). This difference comes from the important reduction of the gas flow towards the side channel using inversely inclined slots.

Those two ledge profiles can also be seen as the extremes of the "anodic cycle-long sidewall temperature peaks" dynamics, the thinner ledge obviously corresponding to higher sidewall temperatures. This drastic thermal impact of the horizontal slots in AP6X technology is in line with the predictions made in recent modelling works linking the gas flow evacuation with the cell thermal balance and sidewall ledge protection [5, 8, 9].

3.2 Impact of the Slot Inclination Angle: From 5 ° to 1.5 °

After a few anode cycles at line amperage in early 2022 to test anodes with 5 ° inclined slots on booster cells, the booster unit was turned on and the amperage brought to its target (see Figure 2). Four different 40 day-long periods were identified to represent steady operation with each type of anode slots and to compare them:

- Horizontal slots at high amperage, from early March 2021 (P1 in Figure 9);
- Inclined slots of 5 ° at line amperage, from early February 2022 (P2 in Figure 9);
- Inclined slots of 5 ° at high amperage, from early July 2022 (P3 in Figure 9);
- Inclined slots of 1.5 ° at high amperage, from early November 2023 (P4 in Figure 9).

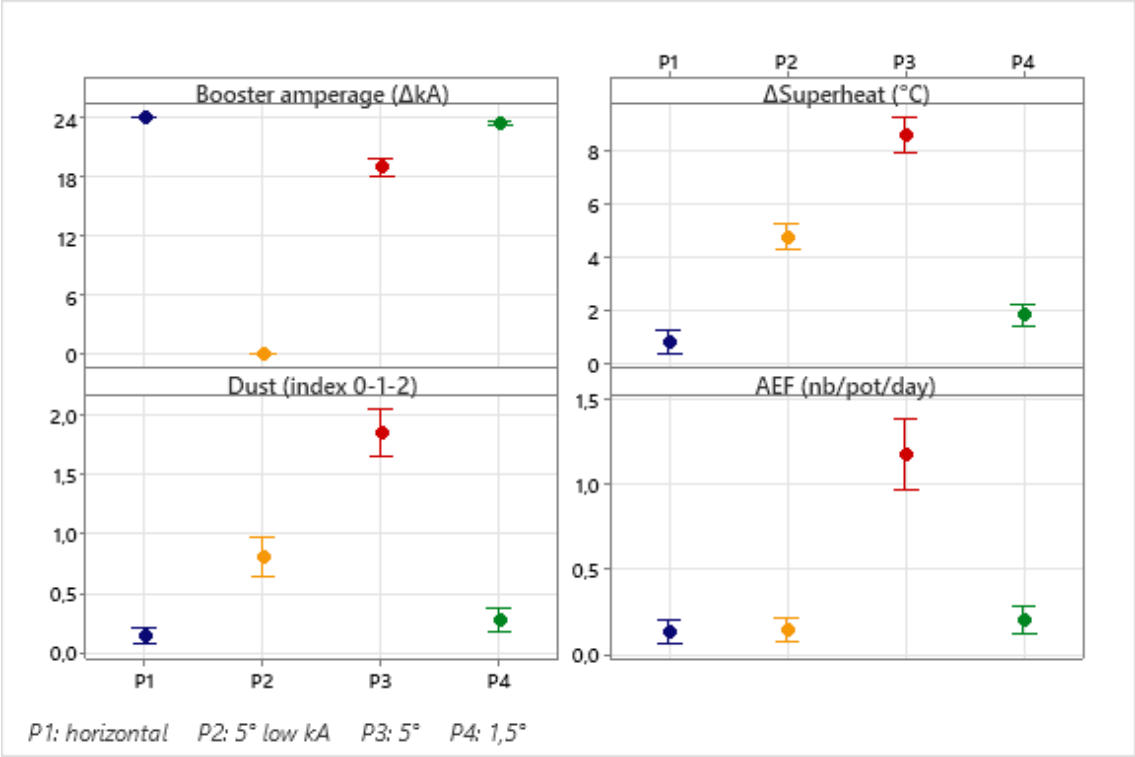

it

Figure 9. Key Process Indicators for the booster cells during the trial.

To illustrate the behaviour of the cells during these periods, a few Key Process Indicators (KPI) were chosen: the amperage, the bath superheat, the dust index, and the anode effect frequency. Two of the indicators are expressed as differences: the amperage and the bath superheat, comparing booster values against line values. For the anode effect frequency, the performance of the AP6X cells is reported directly ("NTEA" values, or *Nombre de Traitements d'Effets d'Anodes - Number of anode effect treatments*, taken from Alpsys® database). The last KPI, the dust index, comes from daily observations made by the R&D technicians at the cell's tapping hole; it is thus an arbitrary evaluation

of the presence of carbon dust on the bath surface. These process indicators are regrouped in Figure 9 for the four 40-day periods.

It is seen that the KPIs of periods P2 and P3, for 5° slots, stand apart. Effectively, even at line amperage (P2), more dust was observed in the cells, which had higher superheat, roughly +4 °C. Increasing the amperage (P3) made things worse, as the superheat increased by a further +4 °C (making it roughly +8.5 °C compared to line cells). Indeed, period P3 corresponds to the "Crisis" presented earlier on the timeline of Figure 2, which also stands out with its very high anode effect frequency, around 1.1 AE/cell/day (AE: Anode Effect). This crisis was serious enough, with very dusty pots and very high superheat, that it led to multiple anode incidents (so-called "mushrooms"), and then to the fallback position of shutting down the booster unit and removing the 5 ° inclined slot anodes to replace them with horizontal-slotted anodes temporarily.

3.2.1 A Deeper Look at the Failure of the 5° Slots

The crisis that ensued from operating the booster section with 5 ° inclined slots at high amperage led R&D teams to realize how this slot design undermined the process performance. A few plausible assumptions were brought forward to put the team into action and make the necessary verifications:

1. Gases channeled through the inclined slots while they are partially immersed are propelled onto the anode facing the slots' exits in the central channel.
2. Gases travel longer distances inside inclined slots, causing erosion of the inner surface of the slots.

To test these assumptions, anode assemblies were taken out of the cells at the corresponding moment of the anode life, and the results are presented in the next two figures. Figure 10 illustrates the first mechanism, when an anode with partially immersed slots ejects gases onto the opposite anode. No damage whatsoever was observed on any of the six "opposite" anode assemblies taken out of the booster cells to verify this assumption; hence, this mechanism did not come into play in the crisis.

Figure 10. Assumption of gases from inclined slot impacting the anode across (left – schematic representing the assumed phenomena; right – anode assembly taken out of a cell, corresponding to the right-hand-side anode block of the schematic).

Figure 11 shows that 3D scans of anode bottoms were performed to look at inclined slot geometry at slot mid-life. The scans did indicate a small enlargement of the inclined slots, towards the central channel exit, a phenomenon that was not observed for horizontal slots. However, the magnitude of the phenomena observed is not compatible with the importance of the crisis encountered in the booster section.

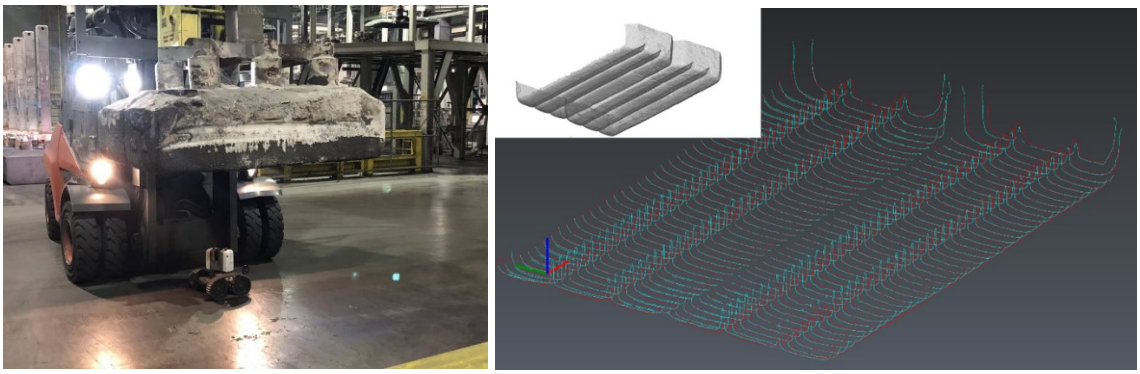

Figure 11. 3D-scan of anode bottom at slot mid-life, to look at slot enlargement from preferential gas evacuation (left – 3D scan of anode bottom; right – slices through the clouds of points to display slot contours at mid-life).

Another assumption, which has not been verified up to now, relates to the transition the anode goes through with inclined slots, which does not happen with horizontal slots. Effectively, with horizontal slots, the anode assemblies around the cell either have slots (younger anodes) or do not have slots (older anodes). In the case of inclined slots, the population is divided in three: a part of the anode assemblies has full length slots, another part has no slots left, but there are also anode assemblies with different slotted lengths. This interesting case is illustrated in Figure 12. It is understood that such a partially slotted anode is a combination of two completely different behaviors: as the unslotted area grows, it enables the coalescence of larger gas bubbles, which are associated with a more unstable, noisy signal of the anode / cell, while the slotted end brings lower noise and cell instability. Furthermore, the higher the slots, the longer this transition lasts (more than three times longer for 5° slots than for 1.5° slots in the case of the AP6X cells), and a greater the number of anode assemblies are affected within the cell at any given time.

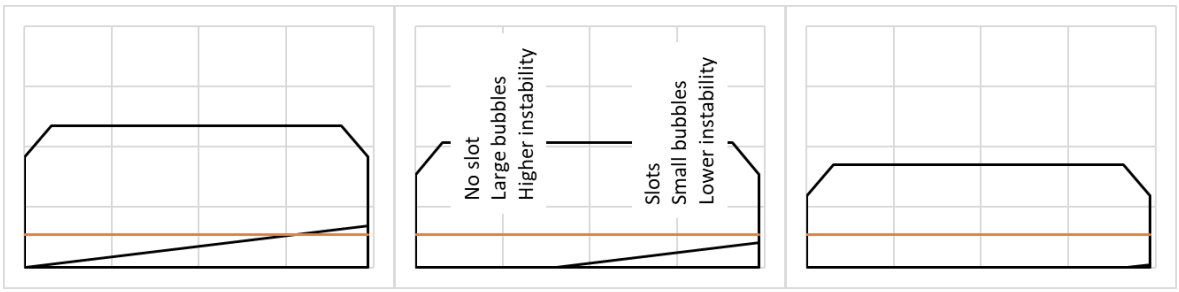

Figure 12. Inclined slots' disappearance and concurrent evacuation modes of the gas bubbles.

3.2.2 Chosen Design: the 1.5 ° Inclined Slot

As mentioned on the timeline of Figure 2, workshops were carried out with R&D teams to find a better anode slot design, from the premises that the ° angle was too steep, and that horizontal slots remained inadequate as they caused recurrent red spots on AP6X shell sidewalls. A minimum angle was sought which would ensure a diminution of the heat transfer to the inner sidewall (as with the 5° slots), but without the process drawbacks previously experienced with inclined slots. An internal CFD modelling study has shown that at angles slightly above 1 °, most of the gases are collected by the slots and directed towards the cell center. An angle of 1.5° was thus retained, which is of the same order of magnitude as the industrial slot angles the authors could find in the literature.

Coming back to Figure 9, it should be mentioned again that until red spots started appearing on the shell sidewalls of booster cells in early 2021, most KPIs were on target, and the AP6X cell technology validation was expected to be completed in early 2022. This situation helps appreciate the closeness between the KPIs of periods P1 and P4, strongly supporting the 1.5 ° inclined slot design solution. This solution is a great improvement which completely settles the problem of recurring red spots on the AP6X platform; however, the state of knowledge on such inclined slots is not advanced enough to declare the 1.5° angle an optimum.

3.2.3 Thermal Impact of Inclined Slots

Reconsidering Figure 9 again, it is seen that with 1.5° slots, the booster cells superheat is higher than with horizontal slots of similar height (roughly +1.5 °C at the same amperage and target resistance). This is an indication of the thermal impact of inclined slots, which lower the heat transfer in the lateral channels. This means that a cell with inclined slots has a lower heat dissipation capacity than its horizontal slots counterpart, and thus must be compensated, by either lowering its power (within acceptable cell instability limits) or increasing its overall heat losses, to maintain its thermal equilibrium (through bath superheat). In the context of this technology development, AP6X cells are operating at higher amperage and lower ACD than the rest of the smelter. Therefore, the ACD lever was not used to adjust the thermal equilibrium of the cells. Instead, the cell's heat losses were modified by decreasing the anode cover height in the booster section by 4 cm.

4. Conclusions

This industrial experiment carried out from 2021 to 2024 demonstrates that the life phases of the horizontal anode slot influence the collection and evacuation regimes of the reduction gases generated under the anodes. The phase when the slots are immersed is the most aggressive in terms of degradation of the inner sidewall ledge protection, imposing a high local heat transfer, which represents a risk of cell life loss. This risk is exacerbated by the amount of collected gas and by the proximity of the anodes relative to the cell sidewalls.

An inclined slot directing gases towards cell center effectively avoids periodic attack on the sidewall by reducing bath flow mixing in the side channel. As a result, the protective ledge that covers the sidewall is stabilized and the overall heat dissipation is lowered. This thermal impact must be compensated either by a reduction in power or an increase in overall heat dissipation of the cell: in the AP6X booster trial, anode cover height was decreased to increase heat losses.

A minimum slot angle is required to ensure that bubbles correctly flow towards the cell center. In the AP6X technology, the retained slot angle is 1.5°, determined by modeling and experimentation. At 5° inclination, a significant deterioration in process performance was observed, with bath overheating and heavy presence of carbon dust. An optimum angle might exist, but with the duration and cost of industrial trials, the answer will likely come from future modelling studies. An optimum angle could also be the minimum angle to sustain the "inclined effect", if the driving phenomena leading to the crisis with 5 ° slots arises from the co-existence of two gases evacuation modes (see Figure 12). Nonetheless, in the coming months, the development of anode slots relative to the protection of lining sidewalls will be further developed by Rio Tinto R&D, with the aim to better understand and quantify the thermal impact that needs to be considered for future developments in cell design.

5. References

1. Sándor Ponczák, Lászlo I. Kiss, Sébastien Guérard and Jean-François Bilodeau, Study of the Impact of Anode Slots on the Voltage Fluctuations in Aluminium Electrolysis Cells, Using Bubble Layer Simulator, *Light Metals*, 2017, 607-614.
2. Vanderlei Gusberti and Dagoberto Schubert Severo, Numerical Modelling of Voltage Drop due to Anode Bubbles, *Proceedings of the 41st International ICSOBA Conference*, Dubaï, United Arab Emirates, 5 – 9 November 2023, *Travaux* 52, 1409-1423.
3. Shuiqing Zhan, Yujie Huang, Zhentao Wang, Changfeng Li, Jianhong Yang and Junfeng Wang, CFD Simulations of Gas–Liquid Multiscale Flow Characteristics in an Aluminum Electrolysis Cell with Population Balance Model: Effect of Anode Slot Configuration, *JOM* vol.71, 2019, 23-33.
4. Zhibin Zhao, Dongfang Zhou, Wei Liu, Hongsheng Hu, Yuqing Feng and Zhaowen Wang, Numerical Assessment on Effects of Longitudinal Slots and its Application in Aluminium Reduction Cells, *JOM* vol.72, no.1, 2020, 218-228.
5. Mostafa El Mehdi Brik, Ievgen Necheporenko and Alexander Arkhipov, Impact of Slot Inclination and Thickness on the Distribution of Gas Bubbles Generated Below the Anode, *Proceedings of the 41st International ICSOBA Conference*, Dubaï, United Arab Emirates, 5 – 9 November 2023, *Travaux* 52, 1425-1438.
6. Meijia Sun, Baokuan Li, Linmin Li, Qiang Wang, Jianping Peng, Yaowu Wang and Sherman C.P. Cheung, Effect of Slotted Anode on Gas Bubble Behaviors in Aluminum Reduction Cell, *Metallurgical and Material Transactions B*, 2017, 3161-3173.
7. Geoff Bearne, Derek Gadd and Simon Lix, The Impact of Slots on Reduction Cell Individual Anode Current Variation, *Light Metals*, 2007, 305-310.
8. Shuai Yang, Jie Li, Yujie Xu, Hongliang Zhang, Xiaojun Lv and Ming Jia, A Modelling of Heat Losses in Aluminium Reduction Cell with Slotted Anodes, *Light Metals*, 2014, 667-672.
9. Nadia Chailly, André Augé, Alexandre Masserey, Julien Hess, Jacques Rappaz and Emile Soutter, Alucell Latest Development: Modelling Impact of CO_2 Bubbles and Anode Slot Configuration on Liquid Flows in Hall-Héroult Pot, *Proceedings of the 41st International ICSOBA Conference, Dubaï, United Arab Emirates*, 5 - 9 November 2023, *Travaux* 52, 1439-1452.
10. Steeve Renaudier, Steve Langlois, Benoit Bardet, Marco Picasso and Alexandre Masserey, Alucell: A Unique Suite of Models to Optimize Pot Design and Performance, *Light Metals*, 2018, 541-549.
11. Yves Caratini, Isabelle Mantha, Benoit Bardet, Sébastien Bécasse, Alexandre Blais, Martin Forté and Sébastien Guérard, Modelling and Measurements to Support Technological Development of AP60 and APXe Cells, *Proceedings of the 33rd International ICSOBA Conference*, Dubai, United Arab Emirates, 29 November – 1 December 2015, Travaux 44, 523-532.
12. Sajid Hussein, Nadia Ahli, Khalil Ebrahim, Nabeel Al Jallabi, Vasantha Kumar Rangasamy, Abdulla Habib, Sergey Akhmetov, Abdalla Alzarooni, Konstantin Nikandrov and Alexander Arkhipov, ALBA Potline 6 Operation during Amperage Increase, *Proceedings of the 40th International ICSOBA Conference*, Athens, Greece, 10 – 14 October 2022, *Travaux* 51, 1019-1032.